

## Electronic Structure and Spin Fluctuations in the fcc Fe–Pd System\*

P. Mohn, E. Supanetz and K. Schwarz

Institut für Technische Elektrochemie,  
Technical University of Vienna,  
A-1060, Vienna, Austria.

### Abstract

The electronic structure of the fcc Fe–Pd alloy system is investigated by band structure calculations employing the augmented spherical wave (ASW) method. The three compositions Fe<sub>3</sub>Pd, FePd and FePd<sub>3</sub> are studied assuming the ordered Cu<sub>3</sub>Au and the CuAu structure respectively. The total energy is computed as a function of volume and magnetic moment  $E(V, M)$  by performing fixed spin moment (FSM) calculations for all three systems. The energy surface of Fe<sub>3</sub>Pd shows two minima, a ground state with an average magnetic moment of  $2.01\mu_B$ /atom and a metastable minimum with a very small moment. The intermetallic compound FePd shows the usual behaviour of a strong itinerant ferromagnet with an average magnetic moment of  $1.56\mu_B$ , where iron carries about  $2.8\mu_B$  as for the high-spin state of pure fcc Fe. In FePd<sub>3</sub> the iron states form rather localised bands and the magnetic moment rises to  $3.2\mu_B$ . Inclusion of spin fluctuations allows treatment of the finite-temperature behaviour of such systems. The magnetic contribution to the thermal expansion coefficient at room temperature for Fe<sub>3</sub>Pd is  $\alpha_m \approx -18 \times 10^{-6} \text{ K}^{-1}$ , which largely compensates the positive phonon (Grüneisen) part of  $\alpha$ .

### 1. Introduction

The system Fe–Pd is the 4d analogue to Fe–Ni and Fe–Pt, all of which have been subject to numerous experimental and theoretical investigations over several decades. On the iron-rich side of the phase diagram, these alloys exhibit itinerant magnetism and INVAR behaviour (e.g. Fe<sub>65</sub>Ni<sub>35</sub> or Fe<sub>70</sub>Pd<sub>30</sub>), while with increasing Pd concentration localised moments are found (Wassermann 1990). Anomalies in the thermal expansion have been reported (Kussmann and Jessen 1962) for the INVAR composition near 30 at.% Pd. The system shows a transition at about 25 at.% Pd from the  $\alpha$ -phase (bcc, on the Fe-rich side) to the  $\gamma$ -phase (fcc, on the Pd-rich side) (Raub *et al.* 1963). Experimentally, it is found that Fe–Pd forms a substitutional disordered alloy, where the atoms are randomly distributed on the lattice sites of an fcc lattice (similar to Fe–Ni). Of the three systems Fe–Ni, Fe–Pd and Fe–Pt, only the latter crystallises in an ordered structure. Band structure investigations have been performed, for example, by

\* Paper prepared for the Festschrift Symposium for Dr Geoffrey Fletcher, Monash University, 11 December 1992.

Delley *et al.* (1983) for the Pd-rich alloys, who found localised moments on the iron sites. Very recently, LMTO (linear muffin-tin orbital) calculations for the ordered systems Fe<sub>3</sub>Pd, FePd, and FePd<sub>3</sub> were published with a detailed discussion (Kuhnen and da Silva 1992).

In order to determine the electronic and magnetic structure of the ordered phases, we perform ASW (augmented spherical wave) calculations (Williams *et al.* 1979) analogous to our earlier investigations on the Fe–Ni system (Mohn *et al.* 1991). Our equilibrium results are very similar to the recent LMTO calculations (Kuhnen and da Silva 1992), but in addition to the electronic structure we study magneto-volume effects and possible instabilities. Therefore, we calculate the total energy  $E(V, M)$  as a function of the volume  $V$  and the spin magnetic moment  $M$  by means of the FSM (fixed spin moment) method (Schwarz and Mohn 1984). These quantum-mechanical band structure results are valid at  $T = 0$  and provide the basis for a Landau–Ginzburg model of classical spin fluctuations at finite temperature (Wagner 1989). With this model we study the temperature behaviour of the Helmholtz free energy from which we derive the magnetic contribution,  $\alpha_m$ , to the thermal expansion coefficient, the key quantity for the understanding of the INVAR effect (Wassermann 1990). In the temperature range where INVAR systems show very low thermal expansion, the positive phonon (Grüneisen) part of the thermal expansion coefficient is approximately compensated by a negative magnetic contribution, which originally was attributed to a transition from a high-moment/high-volume to a low-moment/low-volume state as the temperature rises (Weiss 1963). It has been shown that the existence of such a transition between two discrete magnetic states is not a necessary prerequisite and that already a strong magneto-volume coupling is sufficient to explain the INVAR anomalies in Fe–Ni (Mohn *et al.* 1991). In this context the experiments for Fe–Pt at low temperatures by Abd-Elmeguid and Micklitz (1989) are interesting, since these workers found evidence for a pressure-induced transition from a high-moment to a low-moment state. In the present paper we demonstrate that these experimental data can be understood from our results. In addition the reader is referred to a paper by Entel *et al.* (1993), who discuss in detail the various band structure approaches [including Korringa–Kohn–Rostocker coherent potential approximation (KKR-CPA) results] in order to describe the disordered state in the Fe–Ni system.

## 2. Band Structure Results

### (2a) Method of Calculation

We employ the ASW method developed by Williams *et al.* (1979), which is a first-principles method for self-consistently calculating the band structure of solids. The calculations are based on the local spin-density functional theory by which we treat exchange and correlation effects using the parametrisation of von Barth and Hedin (1972) and Janak (1978). The  $\mathbf{k}$ -space integration is carried out for a uniform mesh of 220  $\mathbf{k}$ -points in the irreducible wedge of the first Brillouin zone for Fe<sub>3</sub>Pd and FePd<sub>3</sub>, and a mesh of 550  $\mathbf{k}$ -points for FePd. The matrix elements are constructed using partial waves up to  $l = 2$  (s, p and d states) and including  $l + 1$  correction terms (due to the internal summation over the three center integrals). The calculations are carried to self-consistency, which is monitored by requiring that the site- and  $l$ -projected partial charges converge to

less than  $5 \times 10^{-5}$  electrons. Magnetism is made possible by allowing for spin polarisation.

In our calculations we assume ordered modifications of the Fe-Pd system:  $\text{Fe}_3\text{Pd}$  and  $\text{FePd}_3$  are assumed to have the  $\text{Cu}_3\text{Au}$  structure, where the Cu atoms occupy the face-centred positions and the Au atoms the corners of a fcc cubic unit cell; for  $\text{FePd}$  we choose the  $\text{CuAu}$  structure, in which Cu and Au occupy the two positions in a body-centred tetragonal lattice with a  $c/a$  ratio of  $\sqrt{2}$ . Our assumption of simulating the alloys as ordered phases is justified, since the disordered systems Fe-Ni and Fe-Pd have properties similar to the ordered compound Fe-Pt, so that effects of order-disorder should not play an important role.

**Table 1. Theoretical equilibrium lattice constants and magnetic moments**  
(1 bohr  $\equiv$  0.52918 Å)

System/Structure	$a_0$ (bohr)	$M_{\text{Fe}}$ ( $\mu_{\text{B}}$ )	$M_{\text{Pd}}$ ( $\mu_{\text{B}}$ )
$\text{Fe}_3\text{Pd}/\text{Cu}_3\text{Au}(\text{sc})$	6.943	2.587	0.289
$\text{FePd}/\text{CuAu}(\text{st})$	4.985	2.797	0.326
$\text{FePd}_3/\text{Cu}_3\text{Au}(\text{sc})$	7.319	3.154	0.311

### (2b) Electronic Structure at the Equilibrium Volume

Total energy minimisation with respect to volume determines the ground state, which is magnetic for all three systems. Table 1 summarises the theoretical equilibrium lattice constants and the respective magnetic moments. The Pd moment remains almost constant and is about  $0.3\mu_{\text{B}}$ , whereas the Fe moment is strongly affected by the (first) coordination shell. On the iron-rich side, the magnetic moment of Fe has about the value one would expect for fcc Fe ( $2.6\mu_{\text{B}}$ ) (Moruzzi *et al.* 1986), but with increasing Pd concentration the iron moment rises to about  $3.2\mu_{\text{B}}$ . Delley *et al.* (1983) have shown with their LMTO calculations, that the iron moment remains at this high value, which is in agreement with neutron diffraction data (Cable *et al.* 1963), even when the Pd concentration is increased to  $\text{FePd}_{26}$ . The origin for this peculiar behaviour must be reflected in the density of states (DOS), which we show in Fig. 1. In all three compounds the interaction between Fe and Pd is characterised by spin-up bands, which are completely occupied (making these systems strong ferromagnets) and show common-band rather than split-band behaviour, which partly occurs for spin-down electrons. In all cases where one forms an alloy between a metal with a large spin splitting (Fe) and one with a small spin splitting (Pd), the interaction between the two constituents is weak (strong) for the spin direction for which the energy difference between the corresponding bands is large (small). Such a magnetic interaction was explained by Williams *et al.* (1981) and termed *covalent magnetism*. It is this covalent interaction which also leads to the formation of localised states and respective moments (Kübler *et al.* 1983). This localisation feature is found to some extent for the Pd states in  $\text{Fe}_3\text{Pd}$ , but is quite pronounced for the Fe states in  $\text{FePd}_3$ . In the next section we give a brief description of the equilibrium electronic structure and refer to Kuhnen and da Silva (1992) for additional discussions.

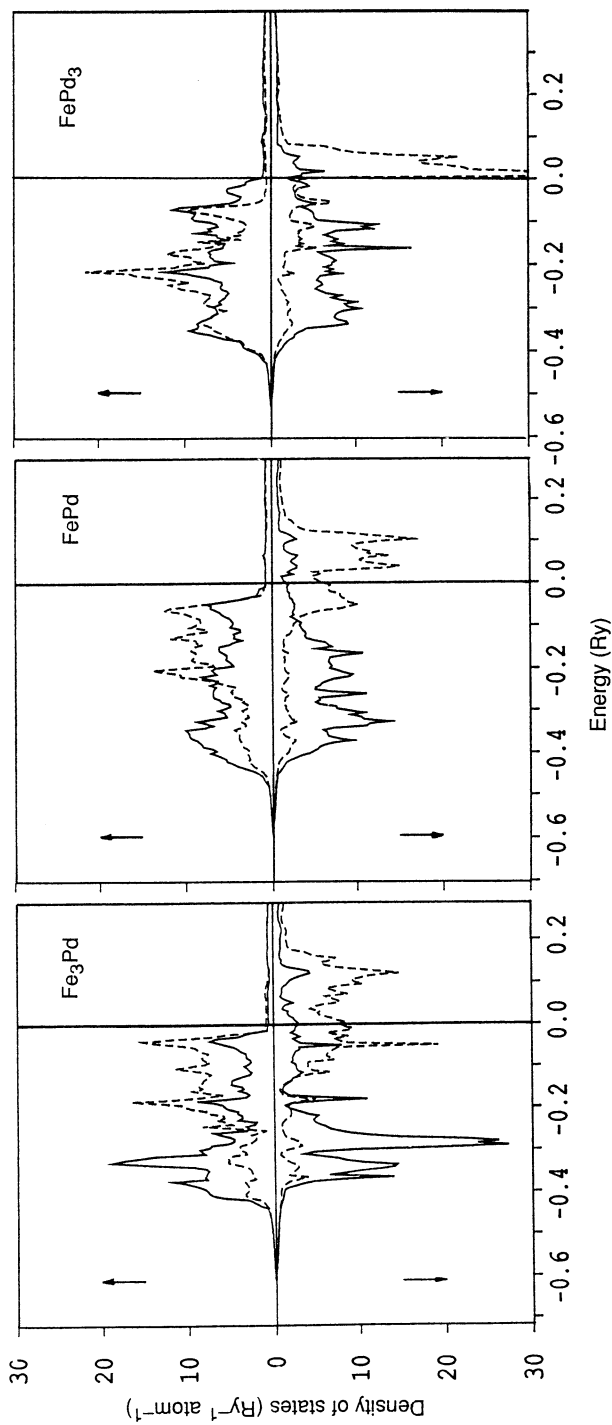


Fig. 1. Spin- and site-decomposed total density of states (DOS) for the three systems investigated. The full curves are the Pd DOS and the dashed curves are the Fe DOS. The energy is taken with respect to the Fermi energy.

**Fe<sub>3</sub>Pd:** The Fe d bands have about the same bandwidth for both spins, with a large band splitting consistent with the magnetic moment of  $\approx 2.6\mu_B$ . The almost completely filled 4d states of Pd form bonding and antibonding states with Fe, where Pd dominates the DOS at low and Fe at high energies, an effect that is even more pronounced for the spin-down bands. The spin polarisation of Pd is caused by the weak *covalent* interaction between Fe and Pd in the spin-down bands, leading to 0.3 unoccupied Pd d states just above the Fermi energy which are responsible for the respective magnetic moment.

**FePd:** The spin-up Pd 4d band is already as broad as in pure fcc Pd, but the d-band width is smaller for the spin-down bands, since interaction with the iron neighbours is reduced. In the Fe-Pd series the Pd states already dominate the electronic structure for FePd, where the repulsive potential of the almost completely filled Pd 4d bands causes the iron states to concentrate near the Fermi energy, especially for the spin-down states.

**FePd<sub>3</sub>:** The electronic structure of this system is very similar to pure fcc Pd. The repulsive interaction caused by the 4d potential is increased with respect to FePd and causes a strong localisation of the Fe spin-down states, which form an impurity peak just above the Fermi energy. The magnetic moment at the iron site is no longer itinerant but shows a more localised behaviour, in agreement with experiment (Wassermann 1990), thus a description in an itinerant electron picture should fail for this system. Here we have an example of a magnetic alloy where the magnetic moment of one constituent is itinerant (Pd) and that of the other is more localised (Fe).

### (2c) FSM Results

In order to obtain a more comprehensive description for the interplay between volume and magnetic moment, we perform FSM calculations which yield the total energy  $E(V, M)$  as a function of volume  $V$  and magnetic moment  $M$ . An analytic expression for this total energy surface is obtained by fitting the numerical results of our band calculations to a polynomial of the form:

$$E(V, M) = AM^2 + BM^4 + CM^6 + \alpha + \beta V + \gamma V^2 + \delta VM^2 + \epsilon VM^4, \quad (1)$$

where the coefficients used are given in Table 2.

**Table 2. Fitted parameters of the energy surface given by equation (1)**

The parameter  $\alpha$  describes a constant energy shift (energy zero) and thus is omitted. The coefficients are chosen such that the energy is obtained in Rydberg units, when the magnetic moment is given in  $\mu_B$ /atom and the volume in bohr<sup>3</sup>/atom

Parameter	Fe <sub>3</sub> Pd	FePd	FePd <sub>3</sub>
$A$	$3.35213 \times 10^{-2}$	$1.69352 \times 10^{-2}$	$2.12515 \times 10^{-2}$
$B$	$-1.92319 \times 10^{-4}$	$2.92756 \times 10^{-3}$	$4.71013 \times 10^{-3}$
$C$	$2.91765 \times 10^{-4}$	$1.09670 \times 10^{-4}$	$-3.99373 \times 10^{-3}$
$\beta$	$-1.87685 \times 10^{-2}$	$-1.66475 \times 10^{-2}$	$-1.42651 \times 10^{-2}$
$\gamma$	$1.22821 \times 10^{-4}$	$9.65384 \times 10^{-5}$	$7.46119 \times 10^{-5}$
$\delta$	$-4.28984 \times 10^{-3}$	$-3.98508 \times 10^{-3}$	$-6.60891 \times 10^{-3}$
$\epsilon$	$-1.33827 \times 10^{-5}$	$8.28233 \times 10^{-4}$	$2.38805 \times 10^{-4}$

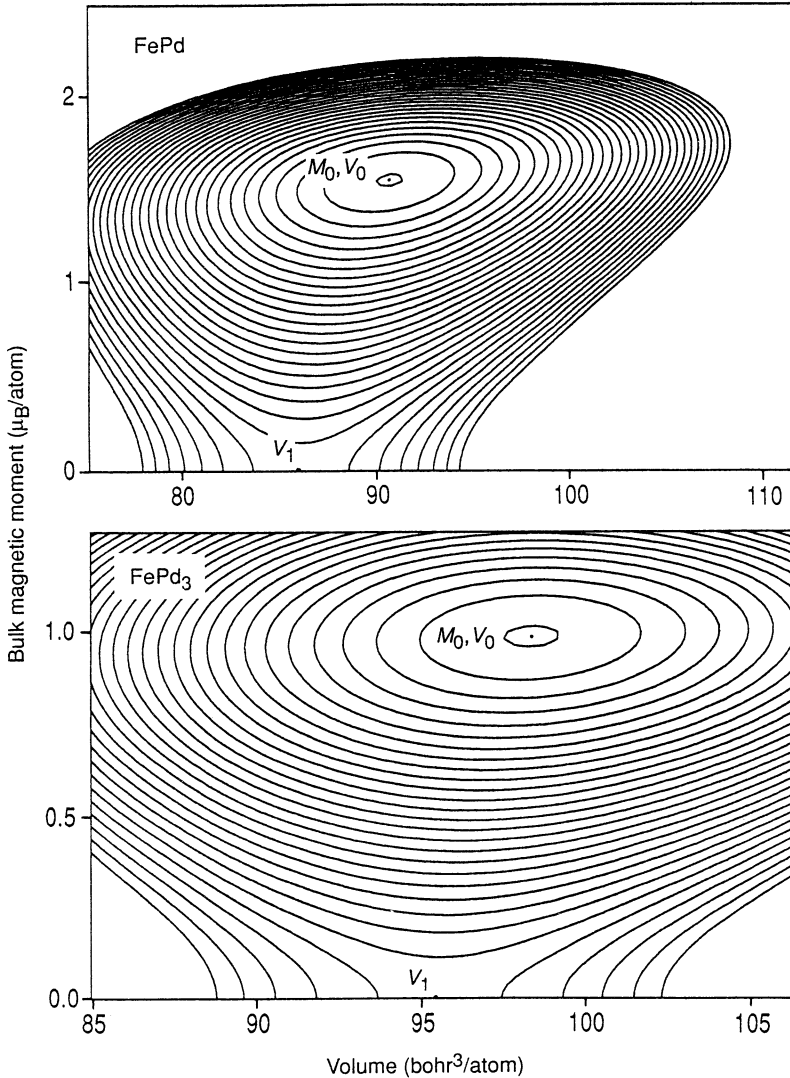


**Fig. 2.** Contour plots of the FSM total energy as a function of volume and magnetic moment for FePd and FePd<sub>3</sub>. All quantities (bulk magnetic moment, volume and total energy) are normalised to one atom. The energy difference between two adjacent contour lines is 1 mRy for FePd and 0.8 mRy for FePd<sub>3</sub>.

Figs 2 and 3 show these FSM surfaces for all three compounds investigated, where for Fe<sub>3</sub>Pd this corresponds to the  $T = 0$  free energy surface (Fig. 3). The finite-temperature results for Fe<sub>3</sub>Pd (also contained in Fig. 3) will be discussed in the next paragraph. The energy surface of FePd shows the usual features of a strong ferromagnet, i.e. a deep minimum and a slowly increasing magnetic moment as a function of volume. The equilibrium ( $M_0, V_0$ ) is stabilised by about 22 mRy with respect to a possible paramagnetic ( $M = 0$ ) state at  $V_1$  and the magneto-volume coupling is small. Although the surface of FePd<sub>3</sub> has a similar shape, the

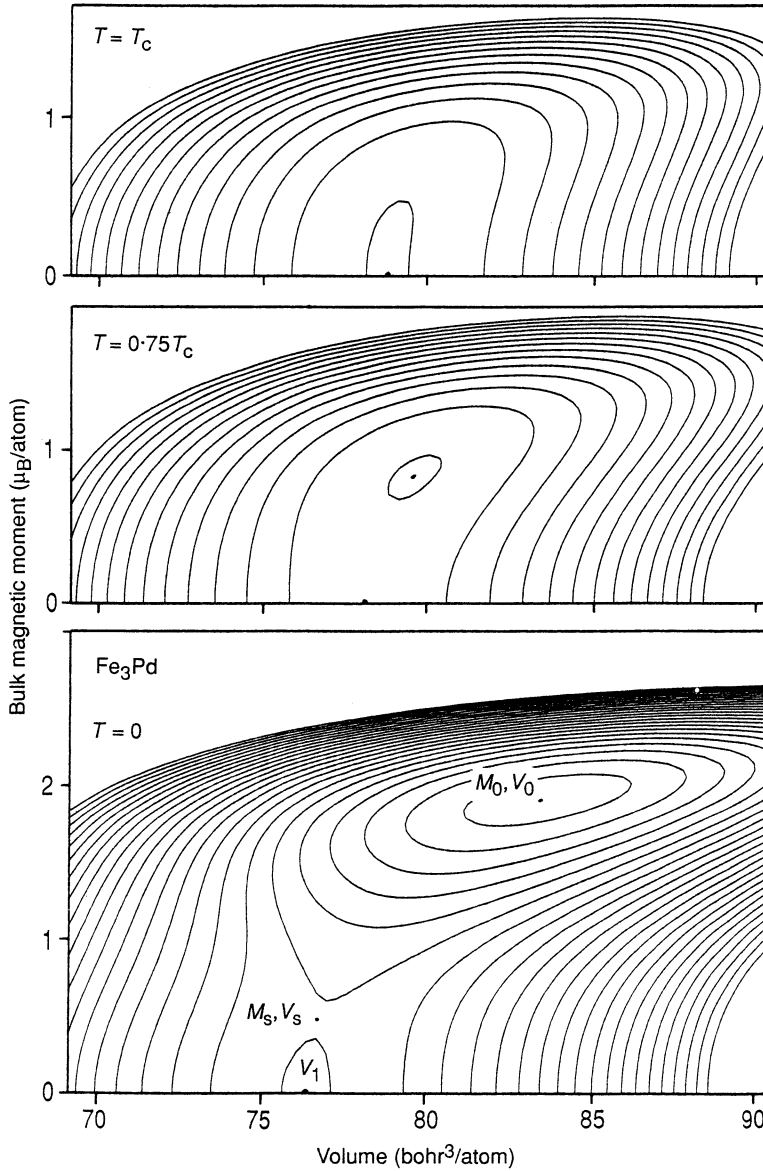


**Fig. 3.** Contour plots of the FSM total energy as a function of volume and magnetic moment for  $\text{Fe}_3\text{Pd}$  (bottom panel). The two panels above show the free energy  $E(V, M, \langle m^2 \rangle)$  at the Curie temperature  $T_c$  and for  $T = 0.75 T_c$ . All quantities (bulk magnetic moment, volume and energy) are normalised to one atom. The energy difference between two adjacent contour lines is 1 mRy.

underlying physics has changed completely. The stabilisation energy is slightly lowered to  $\approx 19$  mRy, consistent with the smaller Curie temperature compared with FePd, but the most interesting feature is the vanishing magneto-volume

coupling which comes from the increased localisation of the Fe moments. Pd has almost filled 4d bands and is a strong ferromagnet in all three compounds, so that it has little flexibility to contribute to a magneto-volume effect. Mainly the Fe states cause such an effect, since they show a large spin splitting and a varying interaction with the Pd states as a function of volume and composition. In  $\text{FePd}_3$ , where the Fe moments are relatively localised, the volume dependence vanishes completely. Moreover, our FSM calculations yield an antiparallel spin alignment between the Fe and Pd moment for small magnetic moments, especially at small volumes.

The most interesting system is  $\text{Fe}_3\text{Pd}$ , for which we find in the  $T = 0$  surface not only the magnetic equilibrium state ( $M_0, V_0$ ; high-moment state), but also a low-moment state with a magnetic moment close to zero (not visible in Fig. 3). The states are separated from each other by a small energy barrier at the magnetic moment  $M_s$  and volume  $V_s$ . This situation resembles somewhat the original suggestion of the  $2\gamma$ -state model by Weiss (1963) who assumed the existence of a high-moment/high-volume and a low-moment/low-volume state. The energy surface of  $\text{Fe}_3\text{Pd}$  shows a much stronger magneto-volume coupling than the other two systems investigated. The magnetic stabilisation energy is lowered to about 6 mRy, but the Curie temperature remains high, namely about 600 K, comparable with that for  $\text{FePd}_3$  of 530 K. This inconsistency between the stabilisation energies and the Curie temperatures suggests that the itinerant picture is valid only on the Fe-rich side, while the localised moments of Fe on the Pd-rich side would require a different (e.g. a Heisenberg) model. In the Fe-Ni system the itinerant picture remains valid over the entire concentration range.

### 3. Effects of Finite Temperature

In order to describe the effects of finite temperatures in an itinerant system one must introduce collective excitations in terms of spin fluctuations (Murata and Doniach 1972). The connection to the FSM energy surfaces was given by Wagner (1989), who formulated a theory for treating spin and volume fluctuations based on a self-consistent Ginzburg-Landau model in which the  $T = 0$  values of the respective coefficients are taken from the analytic expression of the fitted surface according to equation (1).

This model has been successfully applied to describe the finite-temperature behaviour of  $\text{Fe}_3\text{Ni}$  and has explained the anomalous spontaneous volume magnetostriction, which is strongly reduced with respect to the results of the Stoner model based on spin-flip excitations only. In addition, the almost vanishing thermal expansion coefficient has been interpreted as originating from a magnetic contribution that is large around the INVAR composition. A linearised version of this model was applied to the Fe-Ni alloy system by Mohn *et al.* (1991), who found that the dynamical properties of the collective excitations require only one scaling parameter (the average square fluctuations are proportional to temperature), namely the Curie temperature which is taken from experiment. In the original model the scaling was indirectly controlled by a correlation length and a cutoff wavevector for the fluctuations. Further details are given in the

paper by Mohn *et al.* (1991). In the linearised version of the fluctuation model the free energy is written as

$$\begin{aligned}
 E(V, M, \langle m^2 \rangle) = & A(M^2 + 3\langle m^2 \rangle) + B(M^4 + 10M^2\langle m^2 \rangle + 15\langle m^2 \rangle^2) \\
 & + C(M^6 + 21M^4\langle m^2 \rangle + 105M^2\langle m^2 \rangle^2 + 105\langle m^2 \rangle^3) \\
 & + \beta V + \gamma V^2 + \delta V(M^2 + 3\langle m^2 \rangle) \\
 & + \epsilon V(M^4 + 10M^2\langle m^2 \rangle + 15\langle m^2 \rangle^2), \tag{2}
 \end{aligned}$$

where  $M$  is the bulk magnetic moment and  $\langle m^2 \rangle$  is the average square of the local spin fluctuation. In our linearised model the temperature dependence of  $\langle m^2 \rangle$  is given by

$$\langle m^2 \rangle = \langle m^2 \rangle_c T/T_c, \tag{3}$$

where  $\langle m^2 \rangle_c$  is the fluctuation at the Curie temperature  $T = T_c$ , which is (as a ground state property) entirely determined by band structure results by requiring that, at  $T_c$ , both the inverse susceptibility  $\chi^{-1}$  and the bulk magnetic moment vanish:

$$\chi^{-1}(T_c) = \frac{\partial^2 E(V, M, \langle m^2 \rangle)}{\partial M^2} = 0 \quad \text{with} \quad M = 0. \tag{4}$$

This formalism is applied to  $\text{Fe}_3\text{Pd}$  in order to study a possible INVAR behaviour. The free energy  $E(V, M, \langle m^2 \rangle)$  is shown as a function of temperature in Fig. 3, where for  $T = 0.75 T_c$  the bulk magnetic moment (at the minimum of the surface) is about  $1\mu_B$  and the stabilisation energy is below 1 mRy. However, the low-moment state disappears far below  $T_c$ , so that the behaviour of the system at finite temperatures is mainly determined by the strong magneto-volume coupling. At  $T = T_c$  the average bulk moment  $M$  vanishes (by definition) and the free energy surface has a single minimum on the  $M = 0$  axis. With these results we can raise the question of whether or not the existence of two magnetic states is required for the INVAR effect. In  $\text{Fe}_3\text{Pd}$  we found a system which does show two magnetic states at  $T = 0$ , but the low-moment state disappears well below  $T_c$ .

#### 4. Concentration Dependence

The fits according to equation (1) to the three  $T = 0$  energy surfaces shown in Figs 2 and 3 yield seven fit parameters, which vary smoothly as a function of the Pd concentration (Table 2). Since the INVAR properties strongly depend on the concentration of the  $\text{Fe}_{1-x}\text{Pd}_x$  system, we interpolate these parameters between the different ordered phases as a function of  $x$ . For that purpose, we include the fitted values of both pure metals, fcc Fe and Pd (taken from Mohn *et al.* 1991 and Mohn and Schwarz 1992), to have the following five ordered phases for the interpolation: Fe (fcc),  $\text{Fe}_3\text{Pd}$  ( $\text{Cu}_3\text{Au}$ ),  $\text{FePd}$  ( $\text{CuAu}$ ),  $\text{FePd}_3$  ( $\text{Cu}_3\text{Au}$ ), and Pd (fcc). With these data the set of seven parameters can be interpolated as a function of the Pd concentration. This procedure allows us to simulate a continuous variation of the concentration and to determine for each  $x$

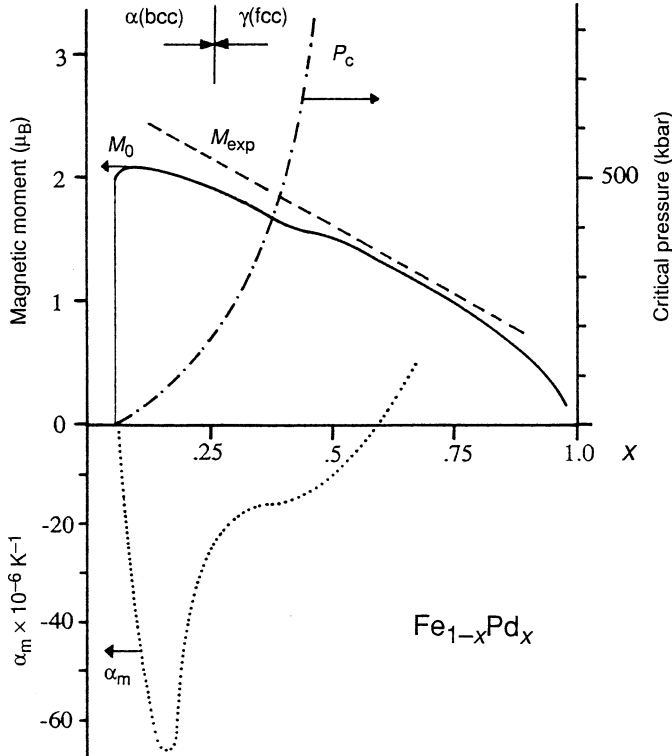


**Fig. 4.** Concentration dependence in the fcc Fe–Pd system: critical pressure  $P_c$  (dash-dot curve; 1 kbar =  $10^5$  kPa), magnetic contribution to the thermal expansion coefficient  $\alpha_m$  (dotted curve), calculated magnetic moment per atom  $M_0$  at the equilibrium volume (full curve), and the corresponding experimental value  $M_{exp}$  (dashed line) taken from Wassermann (1990). We note that Fe–Pd crystallises in the  $\alpha$ -phase (bcc) for  $x \leq 0.25$  and in the  $\gamma$ -phase (fcc) for  $x \geq 0.25$ .

those macroscopic quantities which can be derived from the free energy. The key quantity for the explanation of the INVAR effect, a nearly vanishing thermal expansion coefficient  $\alpha$ , is the magnetic contribution  $\alpha_m$ . As mentioned in the Introduction, in INVAR systems  $\alpha_m$  must be negative and sufficiently large to compensate the positive phonon contribution. At the INVAR composition with  $x = 0.3$  we find  $\alpha_m \approx -18 \times 10^{-6} \text{ K}^{-1}$  (see the dotted curve in Fig. 4), a value that lies in the range found experimentally (Wassermann 1990); towards smaller Pd concentrations  $\alpha_m$  goes through a pronounced minimum around  $x = 0.18$  and finally vanishes, where magnetism disappears. It must be noted, however, that the Fe–Pd system undergoes a transition from the  $\gamma$ (fcc) to the  $\alpha$ (bcc) phase for  $x \leq 0.25$  (see Fig. 4), so that in this concentration range our values correspond only to the hypothetical fcc modification and thus cannot be observed experimentally. Nevertheless, this behaviour is interesting from a fundamental point of view, since this would be a system with a large negative thermal expansion coefficient.

Another crucial INVAR quantity is  $P_c$ , the critical pressure for the disappearance of magnetism, which should be small. It can be calculated by finding the zero of the first derivative of the Gibbs free energy with respect to volume, under the condition that the bulk magnetism  $M$  vanishes. We find that  $P_c$  is small in the INVAR region (Fig. 4) but rises sharply for  $x \geq 0.5$ , i.e. for compositions where  $\alpha_m$  goes through zero and becomes positive. This is the concentration range where the transition from an itinerant model, where spin fluctuation theory is applicable, to localised moments takes place.

## 5. Conclusion

The magnetic and electronic properties of the ordered  $\text{Fe}_{1-x}\text{Pd}_x$  alloy system at  $T = 0$  are calculated by means of the ASW method. The compounds with  $x = 0.25, 0.50$  and  $0.75$  are found to be magnetic at their equilibrium volumes. With increasing Pd concentration the electronic structure gradually changes from an itinerant to a more localised behaviour (with respect to the iron moment), especially for the minority-spin direction. For high Pd concentrations, the magnetic moment of Fe becomes anomalously large, resembling the *giant moment* behaviour found for Fe impurities in Pd (Nieuwenhuys 1975). The FSM total energy surfaces show a coexistence of a low-moment and a high-moment state together with a strong magneto-volume coupling for  $\text{Fe}_3\text{Pd}$ . These results are similar to those for  $\text{Fe}_3\text{Pt}$  for which high pressure experiments (Abd-Elmeguid and Micklitz 1989) show a high-moment/low-moment transition. With increasing Pd concentration the low-moment state disappears and the magneto-volume coupling becomes very small.

The finite-temperature properties are calculated by introducing spin fluctuations via a linearised Ginzburg-Landau model. From the temperature dependence of the free energy surfaces we find that the low-spin state in  $\text{Fe}_3\text{Pd}$  disappears far below the Curie temperature and only the strong magneto-volume coupling remains. From the free energy we also calculate the magnetic contribution to the thermal expansion coefficient which is a large and negative in the INVAR region around  $x = 0.3$ . The concentration dependence of the anomaly in  $\alpha_m$  is even more pronounced than in Fe-Ni, but this feature would occur around  $x = 0.17$  where the fcc phase is no longer stable.

## Acknowledgment

The present paper is dedicated to Dr G. C. Fletcher on the occasion of his 70th birthday. The topic was brought to our attention by Professor E. F. Wassermann, with whom we had many valuable discussions. All calculations were carried out at the IBM ES/9000 computer at the Vienna University Computing Centre under the European Academic Supercomputing Initiative (EASI) sponsored by IBM.

## References

- Abd-Elmeguid, M. N., and Micklitz, H. (1989). *Phys. Rev. B* **40**, 7395.
- Cable, J. W., Wollan, W. O., and Koehler, W. C. (1963). *J. Appl. Phys.* **34**, 1189.
- Delley, B., Jarlborg, T., Freeman, A. J., and Ellis, D. E. (1983). *J. Magn. Magn. Mater.* **31-4**, 549.
- Entel, P., Hofmann, E., Mohn, P., Schwarz, K., and Moruzzi, V. L. (1993). *Phys. Rev. B* **47**, 8706.

- Janak, J. F. (1978). *Solid. State Commun.* **25**, 53.
- Kübler, J., Williams, A. R., and Sommers, C. B. (1983). *Phys. Rev. B* **28**, 1745.
- Kuhnen, C. A., and da Silva, E. Z. (1992). *Phys. Rev. B* **46**, 8915.
- Kussmann, A., and Jessen, K. (1962). *J. Phys. Soc. Japan* **17**, Suppl. B-1, 136.
- Mohn, P., and Schwarz, K. (1992). *J. Magn. Magn. Mater.* **104-7**, 685.
- Mohn, P., Schwarz, K., and Wagner, D. (1991). *Phys. Rev. B* **43**, 3318.
- Moruzzi, V. L., Marcus, P. M., Schwarz, K., and Mohn, P. (1986). *Phys. Rev. B* **34**, 1784.
- Murata, K. K., and Doniach, S. (1972). *Phys. Rev. Lett.* **29**, 285.
- Nieuwenhuys, G. J. (1975). *Adv. Phys.* **24**, 515.
- Raub, E., Beeskow, H., and Loebich, O. Jr (1963). *Z. Metallk.* **54**, 549.
- Schwarz, K., and Mohn, P. (1984). *J. Phys. F* **14**, L129.
- von Barth, U., and Hedin, L. (1972). *J. Phys. C* **5**, 1629.
- Wagner, D. (1989). *J. Phys. Condens. Matter* **1**, 4635.
- Wassermann, E. F. (1990). In 'Ferromagnetic Materials', Vol. 5. (Eds K. H. J. Buschow and E. P. Wohlfarth), p. 23 (North Holland: Amsterdam).
- Weiss, R. J. (1963). *Proc. R. Soc. London* **82**, 281.
- Williams, A. R., Kübler, J., and Gelatt, C. D. Jr (1979). *Phys. Rev. B* **19**, 6094.
- Williams, A. R., Zeller, R., Moruzzi, V. L., Gelatt, C. D. Jr, and Kübler, J. (1981). *J. Appl. Phys.* **52**, 2067.

Manuscript received 4 January, accepted 21 April 1993